

# Photocatalytic oxidation of VX simulant 2-(butylamino)ethanethiol

Alexandre V. Vorontsov<sup>a</sup>, Yi-Chuan Chen<sup>b</sup>, Panagiotis G. Smirniotis<sup>b,\*</sup>

<sup>a</sup> Borekov Institute of Catalysis, Novosibirsk 630090, Russian Federation, Russia

<sup>b</sup> Chemical and Materials Engineering Department, University of Cincinnati, Cincinnati, OH 45221-0012, USA

Received 27 February 2004; received in revised form 4 May 2004; accepted 19 May 2004

Available online 31 July 2004

## Abstract

Photocatalytic oxidation of 2-(butylamino)ethanethiol (BAET) was undertaken in aqueous suspension of TiO<sub>2</sub> Hombikat UV 100 and Degussa P25 under different initial reaction conditions in order to determine the best parameters for the fastest mineralization of the substrate. BAET is considered to be a simulant for the VX chemical warfare agent. The application of ultrasound had only a small positive effect on the BAET photocatalytic degradation. The highest mineralization rate of 0.433 mg/(l min) was found in unbuffered TiO<sub>2</sub> Degussa P25 suspension with initial pH value of about 9.4, TiO<sub>2</sub> concentration 500 mg/l and the initial BAET concentration 1000 mg/l. Decreasing of the initial solution pH to 6.1 or below stops the mineralization of BAET while increasing of pH to about 11 drastically changed the degradation profile. At this initial pH, the first 100 min of reaction led to only oxidation of sulfur moiety and organic intermediates accumulated in the solution. Thereafter, mineralization of the products started. The main detected volatile product was butyl aldehyde and the main polar one was 2-(butylamino) acetic acid. In the case of TiO<sub>2</sub> Hombikat UV 100, conversion of TOC at initial pH 11 exceeded that at initial pH 9.1. For Degussa P25, the starting pH 9.4 was the best for TOC conversion. The results can be used for treatment of water from pollutants with aliphatic nitrogen and sulfur atoms.

© 2004 Elsevier B.V. All rights reserved.

**Keywords:** Photocatalysis; Mineralization; Chemical warfare agents; Ultrasound

## 1. Introduction

Photocatalytic oxidation has attracted increasing attention in view of its high potential for purification of water from various hazardous organic materials [1–6]. Degradation of compounds of different classes – aromatics, chlororganics, alcohols, nitrogen derivatives – was studied relatively thoroughly. Photocatalytic degradation of sulfur and mixed sulfur – nitrogen functionalized organics has not been studied in detail yet. Research with such compounds presents interesting features. First, photooxidating organic sulfur compounds are assumed to form sulfur cation-radicals and their further transformations are of high fundamental interest [7]. Second, recent increased needs of chemical and biological weapons disposal urge the search for advanced methods of their destruction. Chemical warfare agents (CWA) mustard gas (bis(2-chloroethyl)sulfide) and

VX (*S*-2-(diisopropylamino)ethyl *O*-ethyl methylphosphonothioate) are examples of organic compounds containing sulfur and sulfur plus nitrogen atoms, respectively. The principal possibility for destruction of selected CWA into inorganic products by means of liquid-phase photocatalysis was demonstrated before [8]. However, practical application of photocatalytic water purification from CWA requires high mineralization rates. Thus, there is the need to locate the best photocatalyst, pH and optimum concentrations for the fastest water purification from specific pollutants.

There are reports that application of low frequency ultrasound accelerated the photocatalytic mineralization of several compounds including many aromatics [9]. Therefore, one can presume that photocatalytic destruction of CWA simulants could also be accelerated using ultrasonication.

Among other chemical warfare agents, VX is the most difficult for destruction [10]. Three days hydrolysis of VX in water results in only 50% conversion. Application of 0.1 M NaOH makes hydrolysis faster – it is half finished in 31 min. However, a stable byproduct of toxicity equal to that of VX is generated during hydrolysis [10]. Destruction

\* Corresponding author. Tel.: +1 513 556 1474; fax: +1 513 556 3473.  
E-mail address: panagiotis.smirniotis@uc.edu (P.G. Smirniotis).

of VX with hypochlorite requires very big excess of this reagent. The VX in stockpiles is not a pure compound and some impurities like *O,S*-diethyl methylphosphonothioate and *S*-2-(diisopropylamino)ethyl methylphosphonothioate are very toxic. The method of destruction must decrease toxicity of both VX and its impurities in order to be efficient. Due to the low selectivity of photocatalytic oxidation towards substrates it is capable of destroying of almost any organic chemicals including CWA and their impurities [8]. Peroxyacids were recently suggested as nucleophilic agents for decontamination of VX and soman [11]. The enhanced nucleophilicity of peroxyacids afforded efficient split of P–S bond of VX in basic media. The forming products possess much lower toxicity but require further treatment before disposal. Photocatalytic oxidation, however, can be used as a one step process for complete destruction of all diluted warfare agents into inorganic products.

In the present work, we study for the first time the influence of such reaction conditions as TiO<sub>2</sub> photocatalyst type, initial pH of solution, initial concentration of substrate and photocatalyst as well as effect of ultrasound on the rate of photocatalytic mineralization of 2-(butylamino)ethanethiol CH<sub>3</sub>CH<sub>2</sub>CH<sub>2</sub>CH<sub>2</sub>NCH<sub>2</sub>CH<sub>2</sub>SH. This compound contains sulfur and amine atoms and imitates chemical agent VX, which is too toxic for work in civil research environment. The VX molecule CH<sub>3</sub>CH<sub>2</sub>O(CH<sub>3</sub>)(O)PSCH<sub>2</sub>CH<sub>2</sub>N(iPr)<sub>2</sub> contains analogous radical, SCH<sub>2</sub>CH<sub>2</sub>N(iPr)<sub>2</sub>. The VX molecule contains tertiary amine and imitant contains secondary one. Photocatalytic oxidation of tertiary amines proceeds, however, through the formation of secondary amines [12]. Destruction of the mentioned sulfur-containing radical in VX completely removes its toxicity and is a key to VX decontamination [10]. These two facts testify that 2-(butylamino)ethanethiol (BAET) can simulate VX in photocatalytic degradation.

## 2. Experimental

### 2.1. Materials and reagents

TiO<sub>2</sub> powders, Hombikat UV 100 (100% anatase, average particle size 8 nm, surface area 315 m<sup>2</sup>/g [13], produced by Sachtleben Chemie GmbH), Degussa P25 (75% anatase, 25% rutile, primary particles of diameter around 21 nm and surface area of 50 m<sup>2</sup>/g [14], Degussa) were selected as photocatalysts for the study. BAET was supplied by Sigma–Aldrich and used without further purification. Purified water with total carbon content less than 0.5 mg/l and resistivity more than 17 MΩ cm was used for all experiments. For the qualitative analyses of unknown nonvolatile products we used derivatization techniques. Bis(trimethylsilyl) trifluoroacetamide + 1% trimethylchlorosilane (BSTFA + TMCS) was used as the derivatization reagent and was purchased from Supelco. Oxygen (99.5%) was supplied

by Wright Brothers. Buffer with pH 7 containing 0.05 M solution of KH<sub>2</sub>PO<sub>4</sub> and NaOH was a product of Fisher Scientific. Solid phase microextraction (SPME) was carried out using 85 μm Carboxen/polydimethylsiloxane Stableflex fibers installed into manual fiber holder, both supplied by Supelco.

### 2.2. Photooxidation experiments

A 250 ml cylindrical photoreactor having water cooled jacket was used to carry out the reaction at temperature 25 ± 2 °C. A high-intensity medium pressure 450 W UV lamp hosted in a Pyrex jacket (cut-off wavelength 320 nm) illuminated the reactor from the bottom. An ultrasound transducer was dipped into the solution from the top of the reactor and was powered by an UWR ultrasonic processor at amplitude of 50% corresponding to the power input of 65–75 W at the frequency 20 kHz. The sono-photoreactor was housed inside a UV-safety cabinet. Oxygen sparging at a flow rate of 500 cm<sup>3</sup>/min served simultaneously for agitation of suspension and prevented TiO<sub>2</sub> settling in photocatalytic experiments. No substantial organic material removal from suspension by oxygen sparging was noted in all experiments. 100 ml of aqueous slurry containing 250 mg/l TiO<sub>2</sub> and 250 mg/l BAET or other specified concentrations was placed in the reactor. The effect of different concentrations of catalysts and BAET was evaluated in separate experiments. The initial pH of slurry was adjusted using additions of H<sub>2</sub>SO<sub>4</sub> or NaOH. Experiments at pH around 9 were carried out without additions of acid or base. Thus, unadjusted pH was slightly different for different runs. We believe that this small difference has no marked effect on the BAET degradation profiles. The slurry was sonicated for 10 min in an ultrasonic bath. The slurry was stirring for 20 min before and after the sonication. Samples (2 ml each) were withdrawn from the reactor with a syringe, diluted 5 times, and filtered through 0.2 μm polypropylene membrane filters to remove suspended titania particles. Dilution of the samples was necessary to produce enough volume for total organic carbon (TOC) measurements and GC/MS analysis.

### 2.3. Chemical analysis

The TOC concentration in the samples was determined with a Shimadzu TOC-VCSH analyser. The error of TOC measurements was below 5%. For analysis of non-volatile intermediates of BAET degradation, the samples were pre-treated by adding 0.1 ml pH 7 buffer containing 0.05 M solution of KH<sub>2</sub>PO<sub>4</sub> and NaOH, evaporating till dryness, and derivatization for 20 min with BSTFA + TMCS reagent. The formed trimethylsilyl-derivatized products were analyzed by GC/MS Shimadzu QP5050A equipped with a Shimadzu XTI-5 column (30 m, 0.25 mm i.d.). Calibrations for these compounds were not done due to lack of standards. The error of measurements of peak areas is estimated as 10%, and the detection limit is about 10 ppm. The derivatization technique

allowed detecting and identifying all non-volatile products using GC-MS. Volatile products of degradation were analyzed by solid phase microextraction (SPME). The 2 ml samples were vigorously stirred in 4 ml vials during SPME using headspace absorption. Temperature of the samples was kept at about 60 °C. A Supelco Supelco-Q PLOT column (30 m, 0.32 mm i.d.) was used for analysis of volatile products. The error for SPME measurements is usually higher than for traditional injection technique and in our case is estimated as 20%. The pH measurements of samples were performed using a Fisher Accumet 25 pH meter with Accumet electrode.

### 3. Results and discussion

The following parameters were varied in the present study, namely the absence or the presence of ultrasonic irradiation, initial pH of suspension, the type and concentration of TiO<sub>2</sub> photocatalyst, and the initial concentration of BAET. The rates of BAET mineralization obtained under different conditions are summarized in Table 1. These results are illustrated and discussed in more detail below.

#### 3.1. Effect of ultrasound

The highest effect of ultrasonic treatment on BAET photocatalytic oxidation rate was expected for TiO<sub>2</sub> Hombikat UV 100. This TiO<sub>2</sub> possesses the smallest primary particles size of about 8 nm and primary particles are strongly agglomerated into secondary particles of about 1 μm. Most pores in

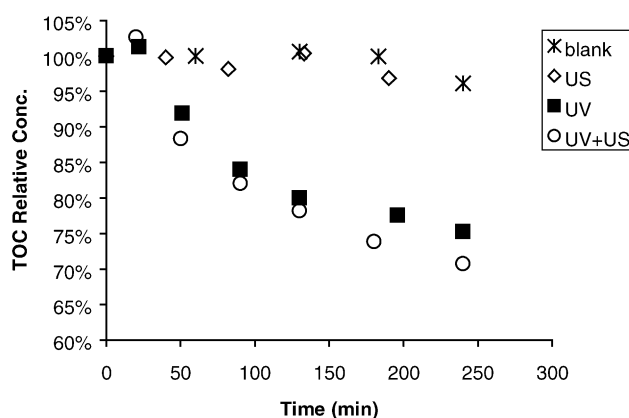


Fig. 1. Curves of total organic carbon (TOC) concentration during degradation of BAET in dark without ultrasonication (blank), with ultrasonication (US), with ultraviolet irradiation (UV), and under ultraviolet irradiation and sonication (UV + US). BAET initial concentration 250 mg/l, TiO<sub>2</sub> Hombikat UV 100 concentration 250 mg/l, starting pH 9.1.

TiO<sub>2</sub> Hombikat UV 100 have diameter of about 4.5 nm [13]. Acceleration by ultrasound can take place via the following effects: inducing chemical transformation by ultrasound itself; increasing available surface area as a consequence of catalyst deagglomeration; enhancing mass transport of reagents to the surface of the catalyst. Fig. 1 shows effect of ultrasound and its influence in the mineralization of BAET in suspension of TiO<sub>2</sub> Hombikat UV 100. Blank run was performed in order to check whether some quantity of organic compounds is removed without ultraviolet irradiation

Table 1  
Summary of BAET mineralization rates under different conditions

Catalyst	Initial pH	Starting BAET concentration (mg/l)	TiO <sub>2</sub> concentration (mg/l)	Ultrasound/UV	Average rate of TOC removal, mg/(l min)	Conversion of TOC within 4 h (%)
Hombikat UV 100	2.0	250	250	UV	-0.022	<1
	4.3	250	250	UV	0.005	<1
	6.1	250	250	UV	-0.014	<1
	9.1	250	250	blank	0.021	4
				US	0.027	7
				UV	0.17	25
				UV + US	0.20	29
	10.2	250	250	UV	0.18	27
	11.0	250	250	UV	0.19	31
	Degussa P25	3.3	250	250	UV	0.023
6.0		250	250	UV	-0.014	1
11.0		250	250	UV	0.22	35
				UV	0.29	43
				UV + US	0.30	45
				UV	0.26	38
				UV	0.33	49
				UV	0.24	35
				UV	0.29	68
				UV	0.37	27
1000	500	500	UV	0.43	17	

and ultrasonic treatment but in the presence of TiO<sub>2</sub>. Oxygen purging is applied during the BAET oxidation in the present study and it could strip away a part of BAET. However, Fig. 1 shows that only a negligible part of organics in suspension, which is within measurements error, is removed in the blank test. The application of ultrasound alone resulted in slight removal of organic carbon from suspension (7% in 4 h), which was also close to measurements error of 5%. Same effect of ultrasound was observed in the presence and absence of TiO<sub>2</sub>. Ultraviolet irradiation of suspension gave rise to 25% decrease of TOC level after 4 h of reaction. Addition of ultrasonication to UV irradiation increased the TOC removal to result in a conversion of about 29% after 4 h of reaction (Fig. 1 and Table 1). Since ultrasound alone does not induce any mineralization of BAET, the influence of ultrasound is limited to suspension deagglomeration and enhancement of mass transport. Our recent study has shown that deagglomeration of TiO<sub>2</sub> Hombikat UV 100 suspension did not increase the rate of mineralization of dimethylmethylphosphonate [15]. Therefore, the observable small additional conversion with ultrasound should be attributed to the enhancement of reagents mass transport to the TiO<sub>2</sub> surface. Most probably, ultrasound enabled transport of reagents into the micropores of this TiO<sub>2</sub>. Table 1 demonstrates that in the case of TiO<sub>2</sub> Degussa P25 there is little effect of ultrasound on the BAET mineralization rate. TiO<sub>2</sub> Degussa P25 consists of primary particles with diameter about 50 nm. The size of the pores is therefore much bigger than in TiO<sub>2</sub> Hombikat UV 100. Mass transport of reagents hardly limits the BAET mineralization rate in P25 in contrast to Hombikat. This explains why the effect of ultrasound is different for these two titanias.

### 3.2. Effect of TiO<sub>2</sub> catalyst type

Two quite different types of TiO<sub>2</sub> were tested for BAET mineralization in the present study. Hombikat UV 100 is 100% anatase TiO<sub>2</sub> with average primary particles size 8 nm and very high surface area of 315 m<sup>2</sup>/g [13]. TiO<sub>2</sub> Degussa P25 is 75% anatase, 25% rutile, has relatively big primary particles of diameter around 21 nm and surface area of 50 m<sup>2</sup>/g [14]. Table 1 allows comparing photocatalytic activity of the two samples in BAET mineralization. In unbuffered suspension with pH around 9, TiO<sub>2</sub> Hombikat has mineralization rate of 0.164 mg/(l min), TiO<sub>2</sub> Degussa has the rate of 0.288 mg/(l min) under the same conditions. The highest activity was observed for Degussa P25, which is speculated to have a very efficient charge separation mechanism at the rutile-anatase interface [14]. The second place is taken by Hombikat. This order of activities is reversed when the samples are tested in gas phase photooxidation, which seems to correlate with surface area [16]. In liquid phase oxidation, diffusion coefficients are several orders of magnitude lower than in gas phase. Therefore, transport of reagents to the photocatalyst's surface can become the rate controlling step. Bigger particle size of Degussa obviously

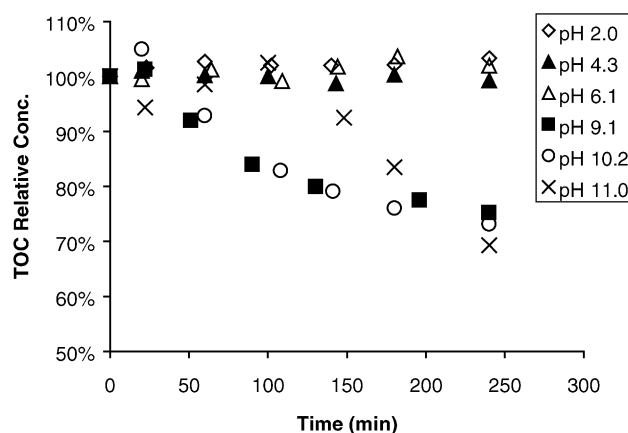


Fig. 2. Effect of initial pH on BAET mineralization curves under UV irradiation over TiO<sub>2</sub> Hombikat UV 100. BAET starting concentration 250 mg/l, TiO<sub>2</sub> Hombikat UV 100 concentration 250 mg/l.

facilitates the transport of reagents to its surface and allows higher reaction rates.

### 3.3. Influence of the Initial pH

As we see, the pH value has significant importance for photocatalytic mineralization of BAET over both Degussa P25 and Hombikat UV 100. The pH of unbuffered suspension containing 250 mg/l of TiO<sub>2</sub> and BAET each amounts 9.1 for TiO<sub>2</sub> Hombikat UV 100 and 9.4 for TiO<sub>2</sub> Degussa P25. The basic pH of the initial solution is due to the basic properties of the secondary aminogroup of BAET ( $pK_a \sim 11$  for secondary amines). The weakly acidic thiol group ( $pK_a \sim 10-11$ ) does not influence pH much. To obtain lower and higher initial pH of suspension, sulfuric acid or sodium hydroxide was added. Fig. 2 represents BAET degradation curves at different pH over TiO<sub>2</sub> Hombikat UV 100. One can observe that at values of pH 6.1 and lower the BAET mineralization completely ceases.

Obviously this can result from the protonation of amino group of BAET at pH values less than  $pK_a \sim 11$  to form  $C_4H_9NH_2^+CH_2CH_2SH$  or its singly protonated dimer  $C_4H_9NH_2^+CH_2CH_2SSCH_2CH_2NHC_4H_9$  that is formed in dark before the start of irradiation [8]. In the case of ammonia photocatalytic oxidation [17], the reaction stopped completely at pH lower than 7.2. The highest reaction rates for those experiments were observed at pH 9.9 or higher. At high pH values, the concentration of protonated ammonia strongly decreases. Thus, the rate of ammonia species oxidation can be correlated with concentration of non-protonated NH<sub>3</sub>. It should also be the case for BAET photocatalytic oxidation. Protonation of BAET happens at higher pH values since its  $pK_a$  is higher than that of NH<sub>3</sub> ( $pK_a = 9.25$ ). Protonated molecules of amine are repelled by partially protonated TiO<sub>2</sub> surface and the reaction is retarded.

BAET photocatalytic degradation in suspensions with initial pH 9.1 and 10.2 shows about the same TOC profiles

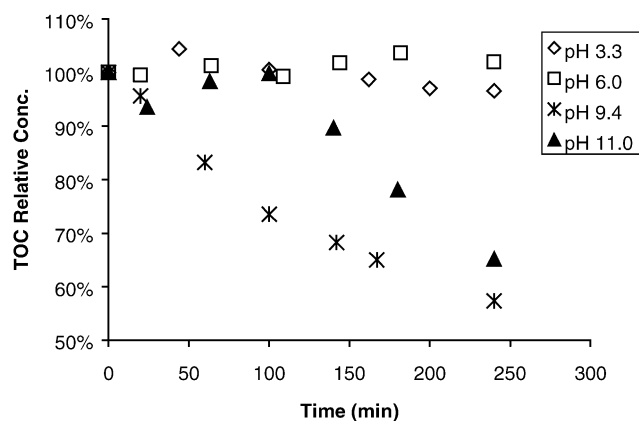


Fig. 3. Influence of initial pH on BAET mineralization under UV irradiation over TiO<sub>2</sub> Degussa P25. BAET starting concentration 250 mg/l, TiO<sub>2</sub> concentration 250 mg/l.

which start to decrease from almost the start of reaction and finally reach conversions 29 and 27%, respectively, after 4 h. The degradation profile at initial pH 11 has the most interesting shape. During the first 100 min of reaction there is no TOC decrease. Thereafter, the TOC starts falling at so high rate that conversion after 4 h (31%) slightly exceeds that for the case of initial pH 9.1 and 10.2. The possible reasons for this behavior are discussed at the end of this section.

The influence of pH on photocatalytic oxidation of BAET over TiO<sub>2</sub> Degussa P25 is shown in Fig. 3 and demonstrates the same tendencies. However, conversion of TOC was considerably higher. The TOC decrease at pH 3.3 and 6 is negligible during the 4 h of reaction. The pH of TiO<sub>2</sub> Degussa P25 suspension without pH adjusting is higher than that of TiO<sub>2</sub> Hombikat UV 100 and amounts 9.4. Hombikat has

about five-fold higher surface area that obviously hosts more acidic OH groups thereby buffering the suspension more effectively. Degradation of TOC at the starting pH 9.4 over Degussa is considerably faster producing TOC conversion 43% after 4 h. The degradation at starting pH 11 shows no TOC conversion during the first 100 min and then the conversion starts at a higher rate than that at starting pH 9.4. However, conversion after 4 h is markedly smaller than conversion at pH 9.4 (Table 1). Comparing TiO<sub>2</sub> Degussa and Hombikat one can observe that TiO<sub>2</sub> Degussa provides about 14% higher conversion at the best pH and thus is more suitable for water purification.

The observed dependence of BAET degradation on initial pH can be viewed as superposition of dependencies for mercaptans and amines. The pH dependence for amines increases with increased pH and stay constant at pH above 9. The dependence of photocatalytic degradation rate of several aromatic mercaptans on pH was demonstrated to acquire a maximum at pH around 9 [18]. At pH higher or lower, the rate decreases. Thus, the sum of dependencies gives maximum rate at pH around 9 and very slow conversion at lower pHs.

#### 3.4. Behavior of degradation products

Detected volatile compounds are listed and compared for different conditions in Table 2. Several compounds were present in reaction mixture initially. The fact that they are products follows from their higher concentration at some time periods during the reaction. The major volatile product was butanal. Its toxicity is low (LD<sub>50</sub> peroral for mouse 2488 mg/kg) especially when compared to extreme toxicity of VX (LD<sub>50</sub> intravenous for rabbit 0.008 mg/kg). Other

Table 2

Relative peak areas of volatile products of BAET photocatalytic degradation detected by SPME

Compound name	TiO <sub>2</sub> Hombikat UV 100				TiO <sub>2</sub> Degussa P25				
	pH 9.1				pH 11		pH 9.4		
	UV, 0 min	UV, 100 min	UV, 240 min	UV + US, 240 min	UV, 100 min	UV, 240 min	UV, 0 min	UV, 100 min	UV, 240 min
Acetaldehyde	423	1626	391	420	1219	206	281	706	1217
Acetonitrile	49	96	–	–	125	–	24	148	1582
Carbon disulfide	87	–	137	–	124	–	118	–	–
2-Propanal	89	184	502	100	122	–	–	702	144
Propanal	156	2737	1043	555	4704	1195	46	1970	147
2-Propanone	270	168	194	317	375	360	140	589	1579
Butanal	22323	38339	14337	3878	57171	12217	6978	16713	900
2-Butanone	–	–	–	184	–	–	–	–	–
Ethylacetate	41	–	–	–	116	117	–	149	1269
2-Butenal	–	1037	424	–	658	159	–	423	–
1H-pyrrole	–	48	155	81	23	6	–	224	234
1-Nitrobutane	–	209	143	63	1765	3790	–	693	–
1-Isothiocyanato propane	–	–	–	–	93	–	–	–	–
Diethyldisulfide	344	494	398	532	357	188	126	853	749
1-Isothiocyanato butane	–	–	–	–	86	–	–	–	–
1-Butyl-1H-pyrrole	18	182	116	–	99	–	–	43	–
N-ethyl-N-nitrosoethanamine	69	–	–	–	827	–	–	–	–

organic products also do not possess acute toxicity. Therefore, overall toxicity of BAET degradation products is estimated as low. Ultrasonication during BAET photooxidation resulted in smaller concentrations of volatile organics over TiO<sub>2</sub> Hombikat UV 100. This is in agreement with higher mineralization rate of BAET during ultrasonication.

It is interesting to trace the products in BAET degradation at pH 11. The TOC did not decrease during the first 100 min of reaction. However, the concentration of volatile products increased greatly after 100 min. It demonstrates that reaction did take place. Analysis of non-volatile products showed that BAET quickly transforms into its disulfur dimer in dark before the reaction. All photocatalytic transformations start from it [8]. In samples with initial pH around nine, only traces of non-volatile products were found. When the reaction was carried out at initial pH 11, several non-volatile products were detected in large quantities after 100 min of irradiation. The major product corresponds to CH<sub>3</sub>CH<sub>2</sub>CH<sub>2</sub>CH<sub>2</sub>NHCH<sub>2</sub>COOH. The disulfur starting product was not present. Small quantities of 3-hydroxypropanoic and 3-hydroxybutanoic acids were also detected. After 240 min of irradiation, all these products disappeared. This behavior of degradation products shows that at the initial pH 11, the degradation starts with oxidation of sulfur atoms. After they are oxidized, oxidation of the rest of organic moieties starts and this results in removal of TOC.

### 3.5. Effect of TiO<sub>2</sub> concentration

TiO<sub>2</sub> concentration in the suspension is one of important parameters for optimization of reaction conditions. Since TiO<sub>2</sub> Degussa P25 demonstrated the best performance in BAET oxidation, it was taken for TiO<sub>2</sub> concentration optimization. Fig. 4 shows profiles of TOC concentration during BAET oxidation in suspension with TiO<sub>2</sub> concentration

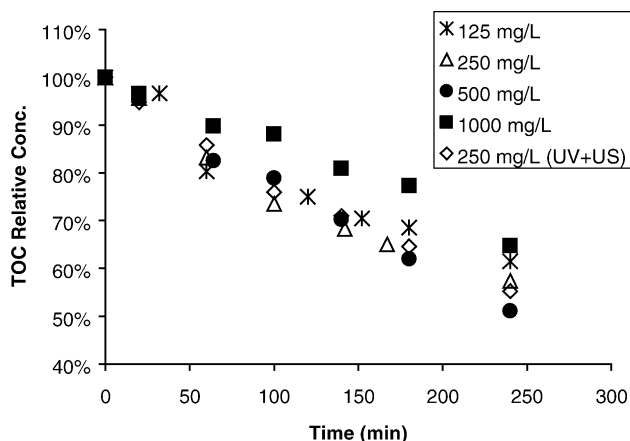


Fig. 4. BAET mineralization curves at different concentration of TiO<sub>2</sub> Degussa P25 under UV irradiation and under UV irradiation and ultrasonication (UV + US). Starting BAET concentration 250 mg/l, initial pH 9.4.

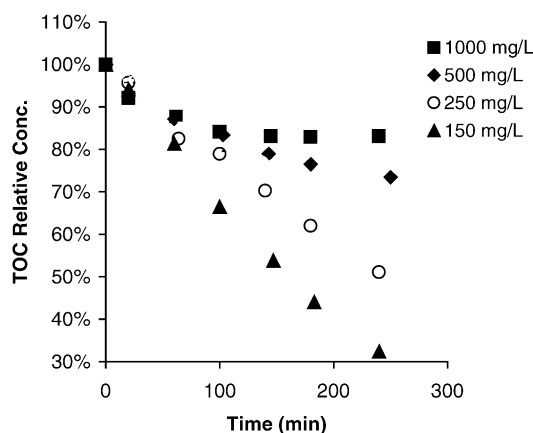


Fig. 5. Influence of BAET starting concentration on its mineralization curves under UV irradiation over TiO<sub>2</sub> Degussa P25. Initial pH 9.4, TiO<sub>2</sub> concentration 500 mg/l.

varied from 125 to 1000 mg/l. The highest conversion of TOC was observed at TiO<sub>2</sub> concentration 500 mg/l. The conversions with concentrations 250, 125, and 1000 mg/l are lower. The optimum concentration of TiO<sub>2</sub> is determined by many factors such as depth of ultraviolet light penetration into suspension, quantity of substrate adsorbed on the TiO<sub>2</sub> surface, size of TiO<sub>2</sub> agglomerates in the suspension, stability of TiO<sub>2</sub> suspension, etc. These factors summed up in the observed experimental dependence that is usually difficult to explain or decouple.

### 3.6. Influence of BAET initial concentration

Photocatalytic degradation usually follows Langmuir-Hinshelwood kinetics [19]. This means that the higher is the substrate concentration, the higher is the reaction rate. Above some substrate concentration the rate usually becomes concentration independent due to saturation of surface adsorption sites. Fig. 5 shows profiles of relative TOC concentration in BAET photocatalytic oxidation with varied initial BAET concentration. TiO<sub>2</sub> Degussa P25 was used because of its highest activity, and TiO<sub>2</sub> concentration of 500 mg/l was employed. The figure shows that the fastest conversion can be obtained at the lowest initial BAET concentration of 150 mg/l. From Table 1, one can see that the rate of TOC consumption increases linearly when initial BAET concentration increases from 150 to 1000 mg/l. Such behavior corresponds to weak adsorption of organics on the TiO<sub>2</sub> surface.

## 4. Conclusions

The best conditions for photocatalytic destruction of VX simulant 2-(butylamino)ethanethiol (BAET) in aqueous solution using particles of suspended TiO<sub>2</sub> have been determined. The highest rate of mineralization was observed at BAET concentration 500 mg/l and TiO<sub>2</sub> concentration 1 g/l.

The mineralization stops completely if the solution of BAET is acidified and proceeds with period of induction if the solution is alkalized.

TiO<sub>2</sub> Degussa P25 demonstrated superior performance with respect to TiO<sub>2</sub> Hombikat UV 100.

### Acknowledgements

We gratefully acknowledge the support of the US Department of Army Young Investigator Program under grant No. DAAD 19-00-1-0399, and NATO Science for Peace Programme via the grant SfP 974209. We also acknowledge funding from the Ohio Board of Regents (OBR) that provided matching funds for equipment to the NSF CTS-9619392 grant through the OBR Action Fund #333. Partial support of Russian Science Support Foundation and grant NSh 1484.2003.3 is acknowledged.

### References

- [1] N.N. Rao, A.K. Dubey, S. Mohanty, P. Khare, R. Jain, S.N. Kaul, Photocatalytic degradation of 2-chlorophenol: a study of kinetics, *J. Hazard. Mater. B* 101 (2003) 301–314.
- [2] M. Hugul, I. Boz, R. Apak, Photocatalytic decomposition of 4-chlorophenol over oxide catalysts, *J. Hazard. Mater. B* 64 (1999) 313–322.
- [3] K.-H. Wang, Y.-H. Hsieh, L.-J. Chen, The heterogeneous photocatalytic degradation, intermediates and mineralization for the aqueous solution of cresols and nitrophenols, *J. Hazard. Mater.* 59 (1998) 251–260.
- [4] J.B. Heredia, J. Torregrosa, J.R. Dominguez, J.A. Peres, Oxidation of *p*-hydroxybenzoic acid by UV radiation and by TiO<sub>2</sub>/UV radiation: comparison and modelling of reaction kinetic, *J. Hazard. Mater. B* 83 (2001) 255–264.
- [5] H.F. Lin, K.T. Valsaraj, A titania thin film annular photocatalytic reactor for the degradation of polycyclic aromatic hydrocarbons in dilute water streams, *J. Hazard. Mater. B* 99 (2003) 203–219.
- [6] S. Rabindranathan, S. Devipriya, S. Yesodharan, Photocatalytic degradation of phosphamidon on semiconductor oxides, *J. Hazard. Mater. B* 102 (2003) 217–229.
- [7] E. Baciocchi, T.D. Giacco, M.I. Ferrero, C. Rol, G.V. Sebastiani, Oxidation of aromatic sulfides photosensitized by TiO<sub>2</sub> in CH<sub>3</sub>CN in the presence of Ag<sub>2</sub>SO<sub>4</sub>. The role of TiO<sub>2</sub> in the chemistry of sulfide radical cations, *J. Org. Chem.* 62 (1997) 4015–4017.
- [8] A.V. Vorontsov, L. Davydov, E.P. Reddy, C. Lion, E.N. Savinov, P.G. Smirniotis, Routes of photocatalytic destruction of chemical warfare agents simulants, *New J. Chem.* 26 (2002) 732–744.
- [9] V. Ragaini, E. Selli, L. Bianchi, C. Pirola, Sono-photocatalytic degradation of 2-chlorophenol in water: kinetic and energetic comparison with other techniques, *Ultrason. Sonochem.* 8 (2001) 251–258.
- [10] Y.-C. Yang, Chemical detoxification of nerve agent VX, *Acc. Chem. Res.* 32 (1999) 109–115.
- [11] T. Cassagne, H. Cristau, G. Delmas, M. Desgranges, C. Lion, G. Magnaud, E. Torreilles, D. Virieux, Destruction of chemical warfare agents VX and soman by  $\alpha$ -nucleophiles as oxidizing agents, *Heteroat. Chem.* 12 (2001) 486–490.
- [12] S. Horikoshi, N. Watanabe, M. Mukae, H. Hidaka, N. Serpone, Mechanistic examination of the titania photocatalyzed oxidation of ethanolamines, *New J. Chem.* 25 (1999) 999–1005.
- [13] A.V. Vorontsov, E.N. Savinov, P.G. Smirniotis, Vibrofluidized- and fixed-bed photocatalytic reactors: case of gaseous acetone photooxidation, *Chem. Eng. Sci.* 55 (2000) 5089–5098.
- [14] B. Sun, A.V. Vorontsov, P.G. Smirniotis, The role of platinum deposited on TiO<sub>2</sub> in phenol photocatalytic oxidation, *Langmuir* 19 (2003) 3151–3156.
- [15] Y.-C. Chen, A.V. Vorontsov, P.G. Smirniotis, Enhanced photocatalytic degradation of dimethyl methylphosphonate in the presence of low-frequency ultrasound, *Photochem. Photobiol. Sci.* 2 (2003) 694–698.
- [16] A.V. Vorontsov, E.N. Savinov, L. Davydov, P.G. Smirniotis, Photocatalytic destruction of gaseous diethyl sulfide over TiO<sub>2</sub>, *Appl. Catal. B: Environ.* 32 (2001) 11–24.
- [17] E.-M. Bensen, S. Schroeter, H. Jacobs, J.A.C. Broekaert, Photocatalytic degradation of ammonia with TiO<sub>2</sub> as photocatalyst in the laboratory and under the use of solar radiation, *Chemosphere* 35 (1997) 1431–1445.
- [18] M.H. Habibi, S. Tangestaninejad, B. Yadollahi, Photocatalytic mineralization of mercaptans as environmental pollutants in aquatic system using TiO<sub>2</sub> suspension, *Appl. Catal. B: Environ.* 33 (2001) 57–63.
- [19] J.-M. Herrmann, Heterogeneous photocatalysis: fundamentals and applications to the removal of various types of aqueous pollutants, *Catal. Today* 53 (1999) 115–129.